



OPEN

SUBJECT AREAS:
BREAST CANCER
TISSUE CULTUREReceived
1 May 2014Accepted
12 August 2014Published
1 October 2014Correspondence and
requests for materials
should be addressed to
B.G. (BGodin@
houstonmethodist.org;
BianaGodinV@gmail.
com)* These authors
contributed equally to
this work.

Three-Dimensional *In Vitro* Co-Culture Model of Breast Tumor using Magnetic Levitation

Hamsa Jaganathan^{1*}, Jacob Gage^{2*}, Fransisca Leonard^{1*}, Srimeenakshi Srinivasan¹, Glauco R. Souza², Bhuvanesh Dave³ & Biana Godin¹¹Department of Nanomedicine, Houston Methodist Research Institute, Houston, TX 77030 USA, ²n3D Biosciences Inc, Houston, TX, 77030 USA, ³Cancer Center of Excellence, Houston Methodist Research Institute, Houston, TX 77030 USA.

In this study, we investigate a novel *in vitro* model to mimic heterogeneous breast tumors without the use of a scaffold while allowing for cell-cell and tumor-fibroblast interactions. Previous studies have shown that magnetic levitation system under conventional culturing conditions results in the formation of three-dimensional (3D) structures, closely resembling *in vivo* tissues (fat tissue, vasculature, etc.). Three-dimensional heterogeneous tumor models for breast cancer were designed to effectively model the influences of the tumor microenvironment on drug efficiency. Various breast cancer cells were co-cultured with fibroblasts and then magnetically levitated. Size and cell density of the resulting tumors were measured. The model was phenotypically compared to *in vivo* tumors and examined for the presence of ECM proteins. Lastly, the effects of tumor stroma in the 3D *in vitro* model on drug transport and efficiency were assessed. Our data suggest that the proposed 3D *in vitro* breast tumor is advantageous due to the ability to: (1) form large-sized (millimeter in diameter) breast tumor models within 24 h; (2) control tumor cell composition and density; (3) accurately mimic the *in vivo* tumor microenvironment; and (4) test drug efficiency in an *in vitro* model that is comparable to *in vivo* tumors.

Development of cancer therapeutics is an ongoing effort by researchers in the academy and pharmaceutical industry. To evaluate optimal dose of therapeutics, conventional two-dimensional (2D) cell cultures are utilized prior to testing on animal cancer models. However, 2D culture models do not mimic the complexity of the tumor microenvironment (tumor stroma). The interactions between the cells and their microenvironment govern various processes, such as cell differentiation, proliferation, and gene expressions in regulation of tumor initiation and progression¹. While animal experiments are necessary prior to any clinical trials, there is a large gap in the knowledge obtained between 2D *in vitro* and *in vivo* models to completely understand the therapeutic efficiency². Data from 2D models rarely predicts magnitudes of therapeutic efficiency *in vivo*. One of the explanations for these discrepancies is the fact that *in vivo* cells are arranged in three-dimensional (3D) structures and not attached to planar surfaces. *In vitro* 3D cultures provide an additional step that can bridge the gap between conventional 2D culture and animal models³. It was shown that *in vitro* 3D cultures enable a better understanding of the molecular and cellular mechanisms, which are more relevant to animal and human studies, thus facilitating the development and screening of new drugs^{2,4}. This affects several aspects related not only to cell-cell interactions, but also to biophysical parameters such as transport of nutrients and therapeutics to different cell populations.

One of the main requirements for a representative 3D *in vitro* tumor system is the presence of a scaffold that can support cancer cells, allow for nutrient, gas, and signal exchanges among cells and mimic extracellular matrix (ECM) conditions. Current scaffolds used are either made from synthetic polymers, such as polyethylene glycol, which is not an appropriate material for cellular recognition, or naturally-derived polymers, such as collagen, which often poses difficulty to produce a controlled matrix⁵. Biodegradable scaffolds have also been tested, but cells may display slow growth and delayed formation of cell-cell interactions, causing a misrepresentation of the *in vivo* environment. Additionally, commercially-available MatrigelTM, is commonly used for 3D culture, which is a reconstituted basement membrane from the mouse Englebreth-Holm-Swarm tumor⁶. Matrigel's animal-derived origins, however, bring concern misrepresenting human tumors and potentially affect experimental results.

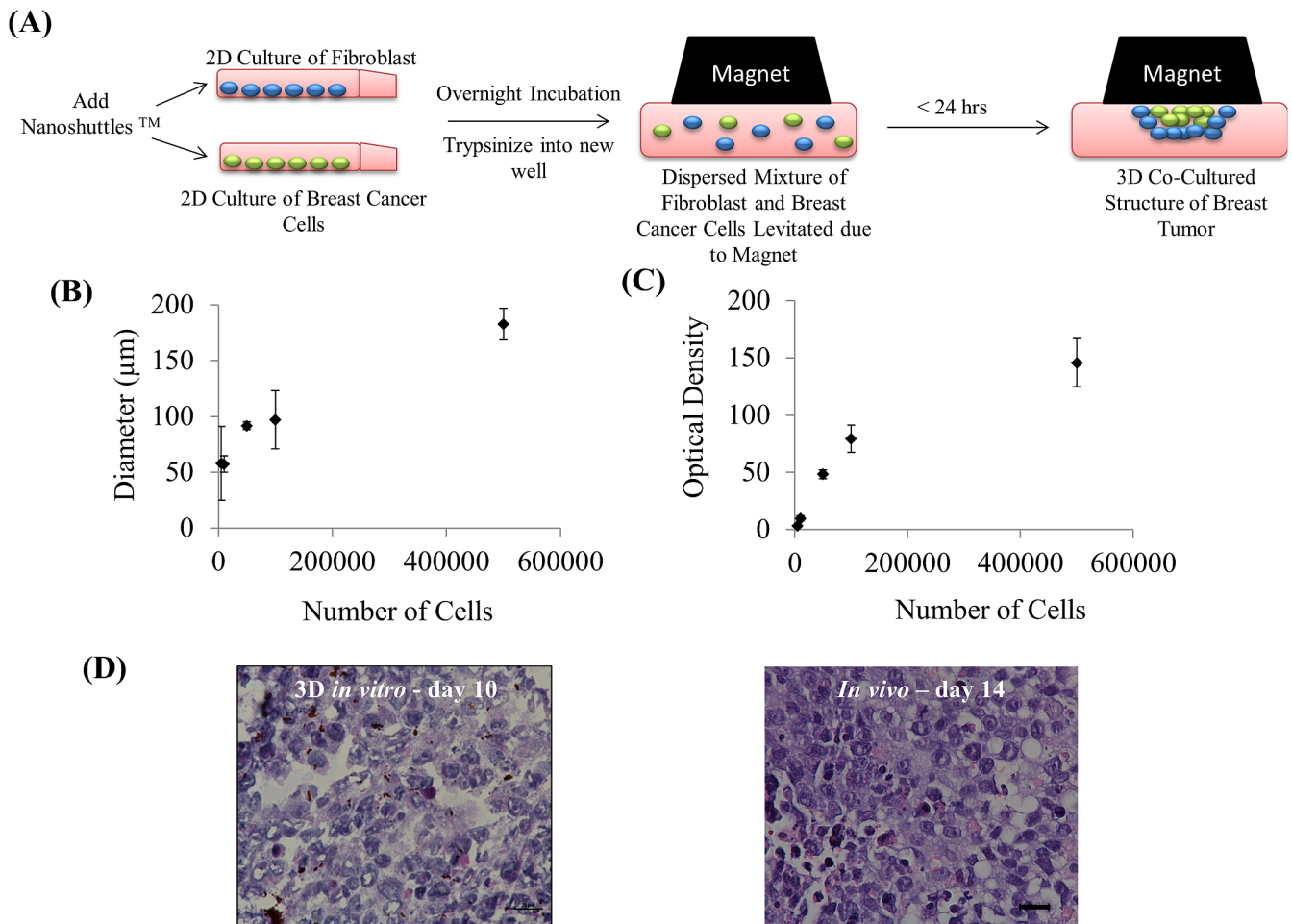


Figure 1 | (A) Schematic representation of the development of 3D *in vitro* breast tumor model from a dispersed mixture of fibroblasts (in blue) and breast cancer cells (in green) after the addition of nanoshuttles. The magnet placed on top aids the attraction of the nanoshuttle internalized cells to form a 3D tumor mass composed of fibroblasts and breast cancer cells and can be grown for several days. (B,C) Plot of the diameter and optical density of 1 day grown 3D *in vitro* breast tumors in 96-well plates, which was measured by GelCount®. (D) H&E staining of 3D *in vitro* tumor models at 50% breast cancer and 50% fibroblast ratio grown in 6 well plates for 10 days comparing to 14 day old *in vivo* mouse breast tumor, Scale bar = 20 µm.

In order to accurately mimic the *in vivo* environment, 3D *in vitro* models without scaffolds have been produced, such as the spheroid model. The spheroid model is a popular approach, especially with breast cancer stem cells, in which cells form heterogeneous aggregates with each other and do not attach to an external surface for support. This model has shown to provide more relevant data than the same cells in the 2D configuration due to the natural formation of cell-cell interactions and the production of tumor-like hypoxia and necrotic regions⁷. The spheroid model, however, does not take into account the presence of and influence from an important tumor component: the stroma.

The breast tumor stroma consists of fibroblasts, adipocytes, endothelial cells, and inflammatory cells with many different enzymes and growth factors, which makes up to 80% of a tumor^{8,9}. Thus the addition of these other cells in an *in vitro* model significantly changes cell-cell contacts and signals within tumors¹⁰. Moreover, the heterogeneous tumor environment affects cell proliferation rates, produces irregular regions of acidity and hypoxia, and influence malignant cell transformations, impacting the sensitivity of tumor to therapeutics¹¹.

In this study, we investigate a novel *in vitro* model to mimic heterogeneous breast tumors without the use of a scaffold while allowing for homotypic and heterotypic cell-cell interactions. Breast cancer cells were co-cultured with fibroblasts and then mag-

netically levitated. It was shown that the conventional culturing conditions using the magnetic levitation system can result in the formation of 3D structures, closely resembling *in vivo* tissues (i.e. adipocytes¹², vascular smooth muscle cells¹³). In this paper, 3D heterogeneous tumor models for breast cancer were designed to effectively model the influences of the tumor microenvironment on drug efficiency. First, the formation of the 3D *in vitro* breast tumor using various breast cancer and fibroblast cell lines were physically characterized (tumor size and density). Then, the model was phenotypically compared to the *in vivo* tumor and examined for the presence of ECM proteins. Lastly, the effect of the presence of a tumor stroma on drug transport and efficiency in the 3D *in vitro* tumor model were assessed.

Results

Fig. 1A schematically represents the step-by-step methodology of formation of 3D *in vitro* breast tumors using a co-culture of breast cancer and fibroblast cells. Breast cancer and fibroblast cells pre-incubated with Nanoshuttles™ were co-cultured at different ratios and magnetically levitated. In less than 24 h, 3D structures containing a mixture of the breast cancer and fibroblast cells were formed. The diameter and optical density of 3D *in vitro* breast tumors were dependent upon the number of cells initially seeded (Fig. 1B, C). It has been previously demonstrated that 3D *in vitro* cultures can be

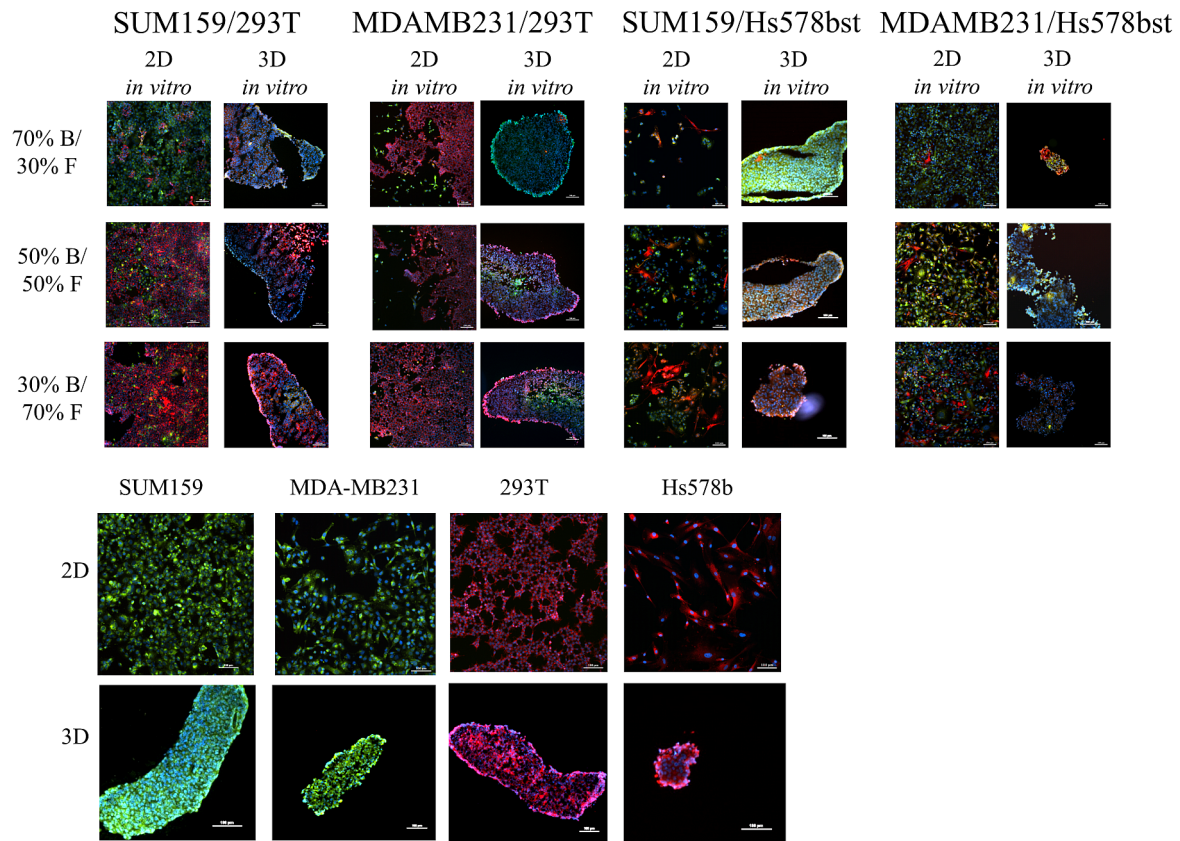


Figure 2 | Comparison of 2D co-culture with the 3D *in vitro* breast tumor model composed with different ratios and types of breast cancer cells (in green) to different types of fibroblasts (in red) grown for 3 days in cell culture conditions (37 C, 5% CO₂). Blue signal is from DAPI, staining the nucleus. Images were taken with 10 × objective magnification, scale bar = 100 μm.

grown for up to 12 weeks using the magnetic levitation system⁶. This 3D *in vitro* breast tumor model with 50 : 50 ratio of breast cancer cells to fibroblasts was also grown for up to ten days with replenishment of cell media. Further, histological analysis has shown that the 3D *in vitro* breast tumor model grown for ten days resembles tumors grown *in vivo* (Fig. 1D). We found that the combination of 70% Fibroblast and 30% breast cancer cell worked the best in the SCID mice model to mimic the condition in human breast cancer which has more stroma than usual breast cancer models in mice (based on clinical samples, data not shown in this manuscript). A few ratios of tumor cells to fibroblasts were injected and, although 293T cells were the fastest dividing cells in *in vitro* system, allowing them to occupy higher volumes after being co-cultured with breast cancer cells, their *in vivo* growth was less prominent when seeded in 50 : 50 ratio. Thus, we decided to compare the above two ratios between *in vivo* and *in vitro* experiments. Both *in vitro* and *in vivo* samples showed disorganized cell structures, which is typical to tumor cells and both featured similar composition of stromal and cancer cells. Similar structures can also be observed in previously published studies *in vivo* with MDA-MB-231 cells¹⁴.

The 3D *in vitro* breast tumor model was compared to the conventional 2D *in vitro* co-cultures with various breast and fibroblast cell lines. Fibroblasts and breast cancer cells were fluorescently labeled with Tracer DiL and Tracer DiO dyes, respectively. Fig. 2 displays the fluorescent images of different cell mixtures grown for 3 days in 2D and 3D configurations. 2D *in vitro* co-cultures of breast cancer and fibroblast cells displayed a dispersed state of growth and attachment, forming a monolayer. 3D *in vitro* model resulted in the formation of tumors with heterogeneous cell distribution and *in vivo* tissue like structure and morphology.

Heterogeneous breast tumors were grown with different ratios of fibroblasts and breast cancer cells using the magnetic levitation system. It is clearly demonstrated that fibroblasts encapsulate breast cancer cells in the 3D *in vitro* system. There is a clear rearrangement of the cells in 3D *in vitro* culture showing a tumor tissue-like organization. This organization is dependent upon specific characteristics of its cellular components. Similarly to *in vivo* situation, the ratio of fibroblasts (red) and cancer cells (green) depended heavily on their nature. It can be seen from Figures 2 and 3 that different cancer cell lines and different fibroblasts vary in their growth patterns and organization, producing heterogeneous *in vitro* tumors. This heterogeneity cannot be seen when the cells were grown in 2D. Moreover, growth rate plays an important role in the formation of 3D tumors *in vitro*. As the fastest growing cell line, samples with 293T cell lines (Fig. 2) were dominated by the fibroblast in most of the combinations tested. Other samples with fibroblasts with slower proliferation rate such as Hs578bst and CAF (Figures 2 and 3) seemed to be growing in sync with the cancer cells and maintained similar ratio to the seeded cells. Primary cancer breast tumor associated fibroblasts, CAF, formed tight spheres with breast cancer cells. Interestingly, all samples with fibroblast cell lines displayed the accumulation of fibroblasts in the periphery region of the spheres, while with the primary CAF cells, the localization of fibroblasts is less pronounced in the periphery. Based on the self-organization of the cells in the produced 3D tumors, in a majority of cases, the concentration of fibroblasts at the tumor edge is substantially higher than in the core, which corresponds to the fibrotic capsule phenomenon observed *in vivo* (Fig. 4A). Additionally, the structure with CAF cells were less organized and formed rough edges of the spheres, showing the slow growing rate of CAF might inhibit the formation of relevant model

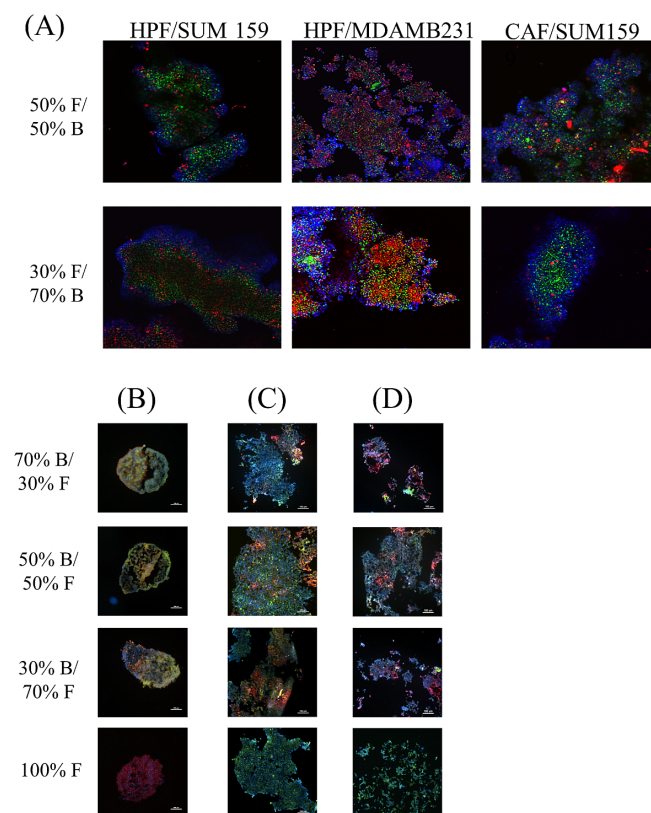


Figure 3 | 3D *in vitro* tumors grown with primary fibroblasts. 3D *in vitro* breast tumor model with different ratios and types of breast cancer cells (green) and primary fibroblasts (red) co-cultured for 3 days using magnetic levitation system. All cells were counterstained with DAPI (blue) for nucleus. (A) Images taken by confocal microscopy of the spheres. (B–D) Fluorescent images of the spheres taken after cryo-sectioning (4 micron slices) (B) MDA-MB-231 and Hs578bst (C) MDA-MB-231 and HPF (D) MDA-MB-231 and CAF. Images were taken with 10 × objective magnification, scale bar = 100 μm.

for *in vitro* spheres. CAF, isolated from tumor lesion of cancer patients and able to secrete relevant factors for tumor survival and growth, is a suitable cell line for modelling fibroblasts in co-culture tumor model. However, the characteristics of slow growth and low availability may limit its utilization for rapid high-throughput assays. The results showed the versatility of the method to obtain various tumor types depending on the cell ratio and the types of cells used in the model, opening the possibility to study heterogeneous tumor types in high throughput system.

The observed fibrotic capsule in 3D *in vitro* tumors expressed different levels of common ECM proteins, such as collagen, vimentin, and laminin (Fig. 4B). Moreover, cells in 3D produced higher concentrations of fibronectin than cells in 2D form (Fig. 4C), providing evidence that co-culture of breast cancer and fibroblasts cells can produce an ECM matrix without a scaffold.

Evidently the density of a tumor can also be controlled by the number of cells initially seeded in to the system. Optical density, or the amount of light that can pass through an object, was used as a parameter to measure tumor density. The darker the tumor appeared in bright field images, a denser tumor can be assumed. Low density tumors were formed by seeding 100,000 cells and high density tumors were formed by seeding 300,000 cells grown for 1 day. To test the penetration of molecules in tumors with different densities, TRITC-tagged dextran (70 kDa) was administered and the change in the TRITC intensity was observed over time. As expected, penetration of dextran through low density tumors was 35% greater than

high density tumors after 2 h (Fig. 5A). Similarly, penetration was studied on tumors grown with low (30% fibroblasts/70% breast cancer cells) and high (70% fibroblasts/30% breast cancer cells) fibroblast content. Penetration through tumors with less fibroblast cells was around 10% greater than tumors with high fibroblast content (Fig. 5B).

To further examine the 3D *in vitro* tumor model as an *in vivo* representation, the penetration and effects of clinically-used anticancer drugs, doxorubicin and Doxil®, was assessed (Fig. 6A). Fluorescent images displayed differences in fluorescent intensity and location of the two formulations within the tumor. Low molecular weight (579 Da) doxorubicin, exhibited higher penetration into the 3D *in vitro* tumor cultures when compared to the 90 nm liposomal formulation of doxorubicin (Doxil®).

Cell viability after doxorubicin/Doxil® treatment was measured using the WST-1 assay (Fig. 6B). For comparison, 2D co-cultures and 3D Matrigel™ mono- and co-cultures were treated for 72 h with the same drugs. Cell viability was normalized to control (cells treated with media alone). Doxorubicin and Doxil® significantly affected the viability in 2D systems when compared to the 3D systems. In both the Matrigel™ and the magnetic levitation system for 3D models, co-cultured tumors treated with doxorubicin exhibited 10% lower overall cell viability when compared to tumors treated with Doxil®.

Tumor area and optical density were measured for monitoring growth of 3D *in vitro* breast tumors in response to doxorubicin treatment (Fig. 7A, B, and C). The area and density for 3D *in vitro* tumors composed of mono- and co-culture of fibroblasts and breast cancer cells increased during the 7 days growth period. On day 7, doxorubicin (100 nM) was added to the 3D *in vitro* mono- and co-cultures. For 3D *in vitro* culture of fibroblasts, the area decreased by 87% for up to 5 days after doxorubicin treatment (from day 7 to day 12). The density, however, did not change after doxorubicin treatment. For the 3D *in vitro* co-culture of breast cancer and fibroblast cells, the area decreased by around 80% and the density decreased by 45% 5 days after doxorubicin treatment. The decrease in tumor size and density after doxorubicin treatment is consistent with *in vivo* findings¹⁵. For the 3D *in vitro* tumor composed of only breast cancer cells, although the area and density changed over time, doxorubicin treatment did not cause additional changes in the tumor area or optical densities.

Discussion

One of the major barriers to the development of efficient cancer therapeutics is the availability of experimental models that can accurately characterize various forms of cancer¹⁶. While animal models have been used extensively, these studies are time-consuming and may not be representative of the human tumors¹⁷. Thus there is a need to develop *in vitro* models that can better represent the human tumors, while still keeping the study times to a minimum. Many three dimensional models have been developed to study cell behaviors such as cell-cell as well as cell-matrix interactions¹⁷. Recently, the tumor-stroma ratio has been found to be a prognostic factor for cancer with higher stromal component contributing to poor prognosis and increased risk of relapse^{18–20}. Thus, it is important to incorporate the stromal components in *in vitro* breast tumor models. Fibroblasts is one of the prominent players in tumor stroma and responsible for secretion of a collagenous ECM and producing different enzymes, inhibitors, growth factors, and structural proteoglycans^{17,21}. Most breast tumors are characterized by loss of epithelial cell polarity leading to a disorganized cellular architecture with randomly interspersed tumor cells and fibroblasts. In this study, we used the magnetic levitation system to mimic this disordered tumor formation *in vitro* by co-culturing breast cancer and fibroblast cells. Additionally, it serves as a versatile tool to form heterogeneous types of 3D *in vitro* breast tumor at various sizes, densities, and compositions by controlling the number and type of cells. Thus, this 3D *in*

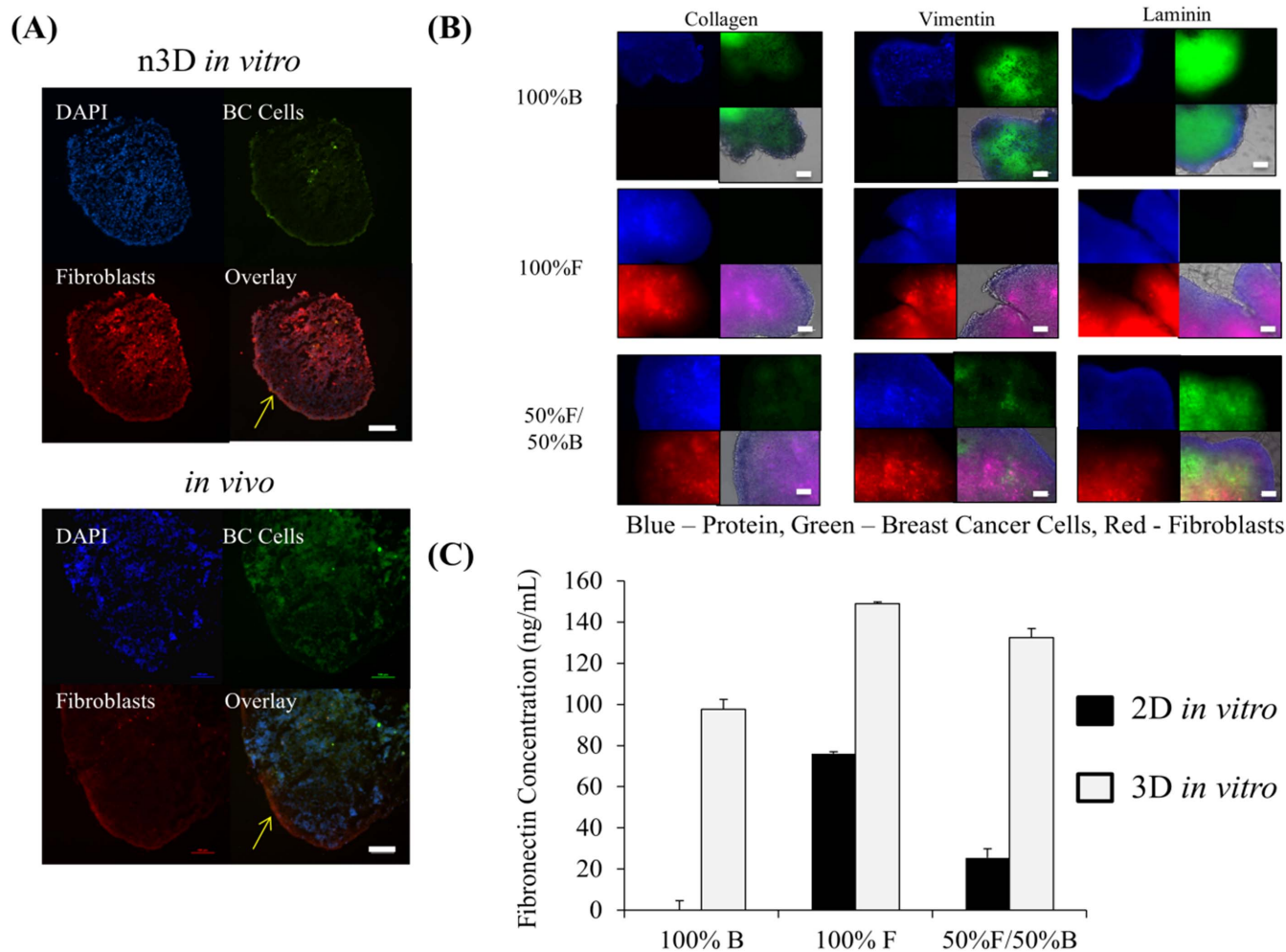


Figure 4 | Characterization of *in vitro* 3D co-cultures: (A) Fluorescent images comparing the phenotype between 3D *in vitro* co-culture grown in 6 well plates and *in vivo* tumors composed of breast cancer cells (green signal) and fibroblasts (red signal) after 7 days growth. Blue signal is from DAPI, staining the nucleus. Yellow arrows indicate the fibrotic capsule formed in both 3D *in vitro* and *in vivo* tumors. Scale bar = 100 μ m. (B) Collagen, fibronectin, and vimentin (in blue) immuno-fluorescent whole mount staining on 7 days old 3D *in vitro* mono- and co- cultures for breast cancer (in green) to fibroblast cells (in red) grown in 24 well plate, overlaid on brightfield image of tumor, Scale bar = 100 μ m (C) Fibronectin concentration detected in 7 days grown 2D and 3D mono- and co-cultures of breast cancer and fibroblasts cells. F = fibroblasts (293T) and B = breast cancer cells (SUM159).

vitro tumor system proves to be an important model to produce breast tumors with different physical characteristics to better understand tumor biology and drug efficiency.

The rate of tumor growth is fast when using the magnetic levitation system compared to the more commonly used 3D cultures formed with MatrigelTM and the tumor forms intrinsic ECM and does not rely on the extrinsic ECM components supplemented to the culture. A tumor structure formed by the magnetic levitation system was observed within 24 h, whereas, the formation of *in vitro* tumor with the same type of cells using MatrigelTM were observed to be slow and delayed and was only comparable after 7 days growth. It has been observed that 3D *in vitro* cultures made with MatrigelTM and other scaffolds take a long time to accurately mimic the *in vivo* tumor phenotypically^{22,23}. Additionally, the cluster size in these slow growing tumor models are generally not large – they are at most in μ m² dimensions^{23–25}. This is important for recapitulating necrotic and/or hypoxic areas in tumors, which occurs only when the tumors are much larger than these dimensions. In the magnetic levitation system, 3D *in vitro* tumors were observed to be in the size range of mm², especially when grown in the 6-well configuration and so can be used to characterize hypoxic regions in the tumor.

Another study has also demonstrated similar formation of large co-cultured tumors of breast cancer in short time scales. However, this model requires the use of an external scaffold to accurately represent the tumor ECM²⁶. While using external scaffolds to mimic the ECM is feasible, and representative for a majority of cell cultures, it may not always accurately characterize the breast tumor. For example, a common scaffold, MatrigelTM, is animal derived and may contain endogenous growth factors and signals that do not represent the human tumor environment. These might have independent effect on the tumors and can affect drug transport and efficiency studies²⁷. More relevant and naturally formed ECM components (collagen, laminin, and fibronectin) provide an advantage over other systems²⁸. In the magnetic levitation system, tumor and fibroblast cells are allowed to interact with each other and naturally form a complex matrix, thus mimicking a more relevant tumor environment without externally-added or other species-derived components.

The presence of ECM in tumors affects drug efficiency due to the molecule's inability to penetrate through the complex matrix and reach the targeted cancer cells¹¹. It has been previously shown that *in vivo* tumors with rich collagen networks inhibited penetration of

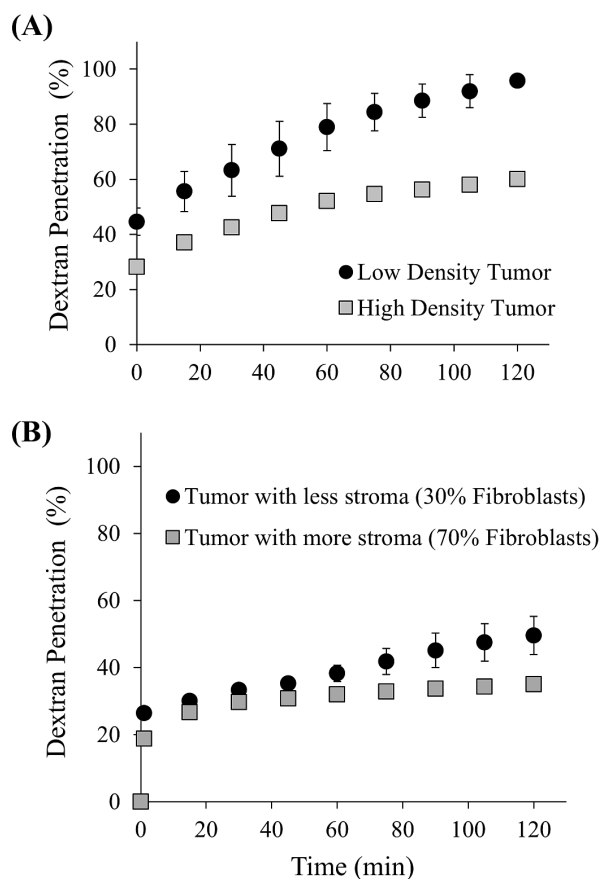


Figure 5 | Penetration of TRITC-tagged dextran: (A) 3D *in vitro* tumors at low and high density tumors (normalized to highest measured TRITC intensity from dextran penetration after 2 hours in low density tumors); (B) 3D *in vitro* tumors with low (30% fibroblasts) and high (70% fibroblasts) stromal content (normalized to TRITC-tagged dextran penetration profile in 3D *in vitro* tumor composed of 100% breast cancer cells (0% fibroblasts)).

high molecular weight drugs when compared to low molecular weight drugs²⁹. Similarly, lower drug penetration was observed in densely packed *in vivo* tumors than in low density tumors¹⁵. The 3D *in vitro* breast tumor made by magnetic levitation system was able to mimic similar physical barriers (stromal composition and density) that are observed *in vivo*. Due to the impaired drug penetration, the cell viability in 3D *in vitro* tumors were not drastically reduced in response to both doxorubicin and Doxil[®] when compared to 2D cultures, in which they showed to cause significant cell death. Similar results of doxorubicin penetrating more through 2D mono-cultures than through 3D *in vitro* mono-culture for liver cancer were reported³⁰. The study attributed the difference in penetration on the presence of ECM. Further, the fluorescent signal from doxorubicin (a small molecule) in the 3D *in vitro* breast tumors was higher than from Doxil[®] (the liposomal form of doxorubicin), confirming that small molecules were able to penetrate better than large drug structures through the 3D *in vitro* breast tumor. Correspondingly, due to the high penetration of doxorubicin in this present study, cell viability of 3D *in vitro* culture treated with doxorubicin was lower than those treated with Doxil[®]. Comparable results were observed in 3D tumors grown using Matrigel[™] system, signifying that either the production or addition of ECM plays an important role in accurately representing drug efficiency under *in vitro* conditions.

In clinical practice, efficiency of tumor therapy is monitored by the tumor size and density over time. The 3D *in vitro* breast tumor model was used to monitor similar physical characteristics of the tumor by

measuring the changes in tumor area and optical density after treatment with doxorubicin for breast tumors *in vivo*¹⁵. While there is evidence that cell viability for mono-culture of breast cancer cells in the 3D *in vitro* tumor model is affected following doxorubicin treatment, it is not reflected in tumor area and optical density. It has been shown that certain tumor cell mono-cultures tend to migrate closer to each other, decreasing in size, when using the magnetic levitation system³¹. The observed decrease in area and increase in density validates that the monoculture of breast cancer cells in the 3D *in vitro* configuration is dominated primarily by migration and therefore, physical changes of the tumor from doxorubicin is difficult to detect using the GelCount[™]. The use of GelCount[™], however, enabled monitoring of growth and physical changes for the most relevant tumor model – the 3D *in vitro* co-culture of breast cancer and fibroblast cells.

In conclusion, taking into account the tumor environmental and physical factors that may impair drug transport are essential for understanding overall drug efficiency. This piece of knowledge is conventionally discovered during *in vivo* animal experiment. To understand drug transportation mechanisms prior to the use of *in vivo* models provides researchers an immense awareness and prediction on drug efficiency. Therefore, the 3D *in vitro* breast tumor model allows researchers to re-create or modify their drug designs prior to initiating expensive, time-consuming animal experiments. The results from this study suggest that the proposed 3D *in vitro* breast tumor is advantageous due to the ability – (1) to form large-sized breast tumor models within 24 h, (2) to control tumor compositions and densities, (3) to accurately mimic the *in vivo* tumor microenvironment, and (4) to test drug efficiency in a more representative model for *in vivo* tumors.

Methods

Materials. Dulbecco's Modified Eagle Medium (DMEM), fetal bovine serum (FBS), and penicillin-streptomycin (P/S) were purchased from Gibco[®] (Invitrogen Corporation, Carlsbad, CA). SUM159 cell line was purchased from Asterand, Inc (Detroit, MI) and MDA-MB-231, Hs785bst, Hs371.t, and 293T were purchased from ATCC (American Tissue Culture Collection, Manassas, VA). Vybrant[™] Cell-Labeling (Molecular Probes) was used to fluorescently label the cells. Breast cancer cells were labeled with Tracer DiO (Em: 501 nm – Green Signal) and fibroblast cells were labeled with Tracer DiI (Em: 665 nm – Red signal) or DiI (EM 565 nm). Nanoshuttles[™] and the Bio-Assembler System[™] were purchased from n3D Biosciences, Inc. (Houston, TX). Doxil[®] was a kind gift from Prof. Y. and doxorubicin and Dextran-TRITC (70 kDa) were purchased from Sigma Aldrich (St. Louis, MO). Matrigel[™] (Basement Membrane Matrix, Growth Factor Reduced (GFR), Phenol Red-Free, LDEV-free) was purchased from BD Biosciences (Franklin Lakes, NJ) and WST1 Solution was purchased from Roche Diagnostics Corporation (Indianapolis, IN). Mammocult media was obtained from Stem cell technologies.

Cell culture. Human Pulmonary Fibroblasts (HPF) SUM159, MDA-MB-231, 293T, Hs785bst and Hs371.t cell lines were cultured in DMEM with 10% FBS and 1% penicillin and streptomycin at 37°C in 5% CO₂ conditions for both 2D and 3D cultures. CAF were patient derived tumor associated fibroblast cells, obtained by mechanical shearing and separation of patient tumors into stromal and epithelial components. The cells were maintained in 50% Mammocult media and 50% DMEM with 10%FBS.

Growth of 3D *in vitro* tumor model. The Bio-Assembler[™] System (in 6-, 24-, and 96- well configuration) from n3D Biosciences, Inc (Houston, TX) was used to construct the 3D *in vitro* breast tumor model. The assembly of 3D *in vitro* cultures was performed as previously reported³². In short, Nanoshuttles[™](NS) were added to cells at a ratio of 1 μ L of NS per 10,000 cells and incubated at 37°C overnight. Cells for 2D and 3D cultures were fluorescently labeled with either Tracer DiO or Tracer DiI (5 μ L dye per 1 ml of media) for approximately 30 minutes at 37°C. The cells for 3D cultures were then detached and co-cultured in the Bio-Assembler[™] system. For example, when using a 24-well ultralow-attachment plate (Corning, Inc. Tewksbury, MA), a total of 100,000 cells were added in each well at different ratios of breast cancer to fibroblast cells in a total volume of 350 μ L of fibroblast medium. Immediately afterwards, a special 24 well lid insert was placed on top of the plate, followed by the magnetic driver which sits inside the insert, and then the 24 well plate on top. The plate was gently shaken to agitate cells and placed in the incubator. After 4 hours, the 24 well plates were briefly observed with bright field microscopy using a 2.5 \times objective to determine if the structures were forming cohesive levitating structures. In brevity, most cells aggregate within a few hours and continue to become denser as more time passes. Fibroblast cells tend to form more dense spheres whereas

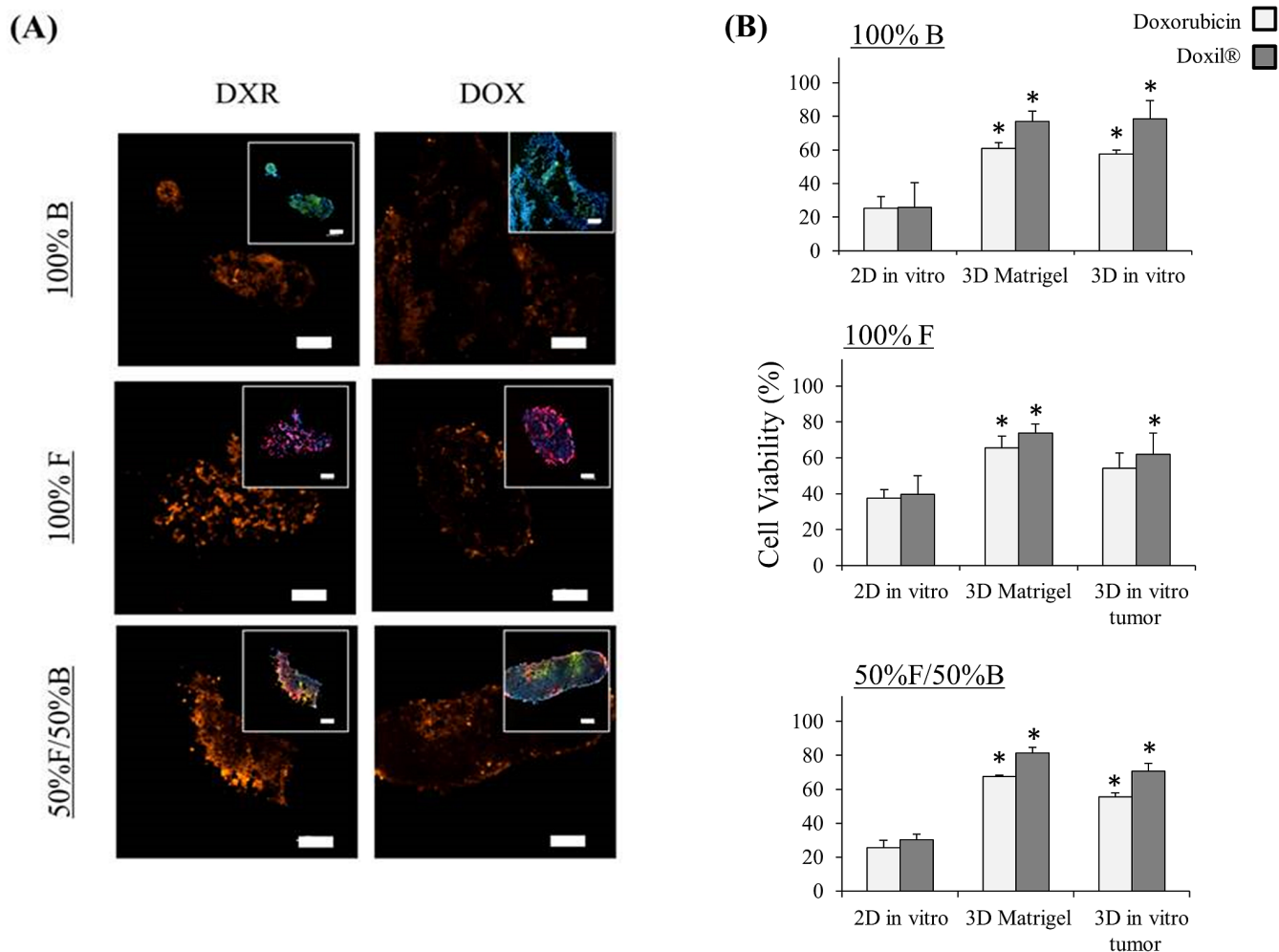


Figure 6 | Distribution and therapeutic efficacy of doxorubicin and Doxil® on 3D *in vitro* tumors: (A) Fluorescent images of 3D *in vitro* tumors composed of mono- or co-culture of fibroblast (in red) and breast cancer cells (in green) –inset images, comparing 72 h treatment with doxorubicin and Doxil®, blue – nucleus and orange – fluorescent emission from doxorubicin, Scale bar = 100 μ m, (B) Viability assay treated with either doxorubicin or Doxil® (100 nM) for 72 h, comparing on three different *in vitro* systems: (1) 2D *in vitro* (grown for 1 day), (2) 3D *in vitro* (grown for 1 day), and (3) 3D Matrigel™ (grown for 7 days) * = statistically significant difference to 2D *in vitro* with the same treatment, $n = 4$, $p < 0.05$. F = fibroblast (293T) and B = breast cancer cells (SUM159).

epithelial-like cells tend to form more sheet like structures and remain flat. After 48 hours, structures from each condition were magnetically removed using a custom magnetic pen (Teflon cap and magnetic cylinder insert), then transferred to cryomolds and were frozen in OCT, cut into 4 μ m sections, and processed for histological imaging. Histological cut and Haematoxylin and Eosin staining was performed by Baylor College of Medicine and Houston Methodist Pathology Cores. 2D co-cultures were cultured on slides and then imaged. The slides were fixed in 4% paraformaldehyde (PFA) for fluorescent imaging. Imaging was performed using the NIKON® Eclipse fluorescent upright microscope at 10 \times magnification.

Whole mount staining for 3D cultures. All immunohistochemistry steps were carried out within a 96 well ultra-low attachment plate while using a custom magnetic plate to hold down 3D cultures during washing and aspiration steps. After being fixed with 4% PFA, all structures were washed with PBS, and then permeabilized with 0.2% Triton-X100 for 10 minutes on an orbital shaker. The structures were then blocked with 10% donkey serum in PBS for 15 minutes and incubated with either mouse anti-collagen type I (Millipore), mouse anti-vimentin (Calbiochem), or rabbit anti-laminin (Abcam) at a concentration of 1 : 100 in PBS with 1% bovine serum albumin overnight at room temperature (RT) while being shaken. The samples were washed and then incubated at RT with either donkey anti-mouse 555 or donkey anti-rabbit 555 (AlexaFluor 555; Invitrogen) at a concentration of 1 : 400 in PBS for 1 h. Samples were washed again and then counterstained with using 4',6-diamidino-2-phenylindole (DAPI; KPL) at 1 : 1000 in PBS. Samples were washed 4 times and kept in PBS until imaged. Imaging was performed using the NIKON® Eclipse fluorescent upright microscope at 10 \times magnification.

***In vivo* tumor sample.** 3–4 weeks old SCID-beige female mice (Harlan) were used as the animal model to grow breast tumors. Fluorescently labeled cells at a ratio of 70%

fibroblasts (293T) to 30% breast cancer cells (SUM159) were injected into the mammary fat pad. After 7 days, tumors were collected, flash frozen in OCT and cut in 4 μ m sections for fluorescent imaging. All animal experiments were performed in accordance to and approved by the Houston Methodist Research Institute, Institutional Animal Care and Use Committee (# AUP-1112-0050).

ELISA. The QuantiMatrix Human Fibronectin ELISA kit (EMD Millipore, Inc., Billerica, MA) with minimum detection limit 10–20 ng/ml fibronectin was used to measure the concentration of fibronectin in 2D and 3D whole cell lysates in *in vitro* cultures. The standards and samples were prepared as per manufacturer's protocol. Samples were used fresh and were diluted at 1 : 10 ratio before the analysis.

Dextran penetration study. The amount of dextran, a model therapeutic agent, penetrating the cultures was studied by measuring the change in TRITC fluorescent intensity over time (0–120 min). 3D *in vitro* tumors formed with different cell numbers and compositions were incubated with TRITC-tagged dextran (70 kDa) for upto 2 h. Time lapse images were taken using the NIKON® Inverted microscope. The change in fluorescence intensity in the 3D cultures was analyzed using the NIS Elements software.

Treatment with anti-cancer drugs. Fluorescently-labeled 3D *in vitro* mono- and co-cultures of breast cancer and fibroblast cells were incubated with doxorubicin or Doxil® (at 100 nM doxorubicin concentration) for 72 h frozen in OCT, sectioned and fluorescently imaged for doxorubicin (Ex: 480 nm/Em: 580 nm). WST1 assay for cell viability was used to examine 2D and 3D *in vitro* systems after 72 h of treatment with either doxorubicin or Doxil®. Briefly, cells were incubated with 10% WST1 solution for 2 h at 37°C and the absorbance at 450 nm was measured. Three dimensional cultures formed using the standard Matrigel™ were compared³³. To

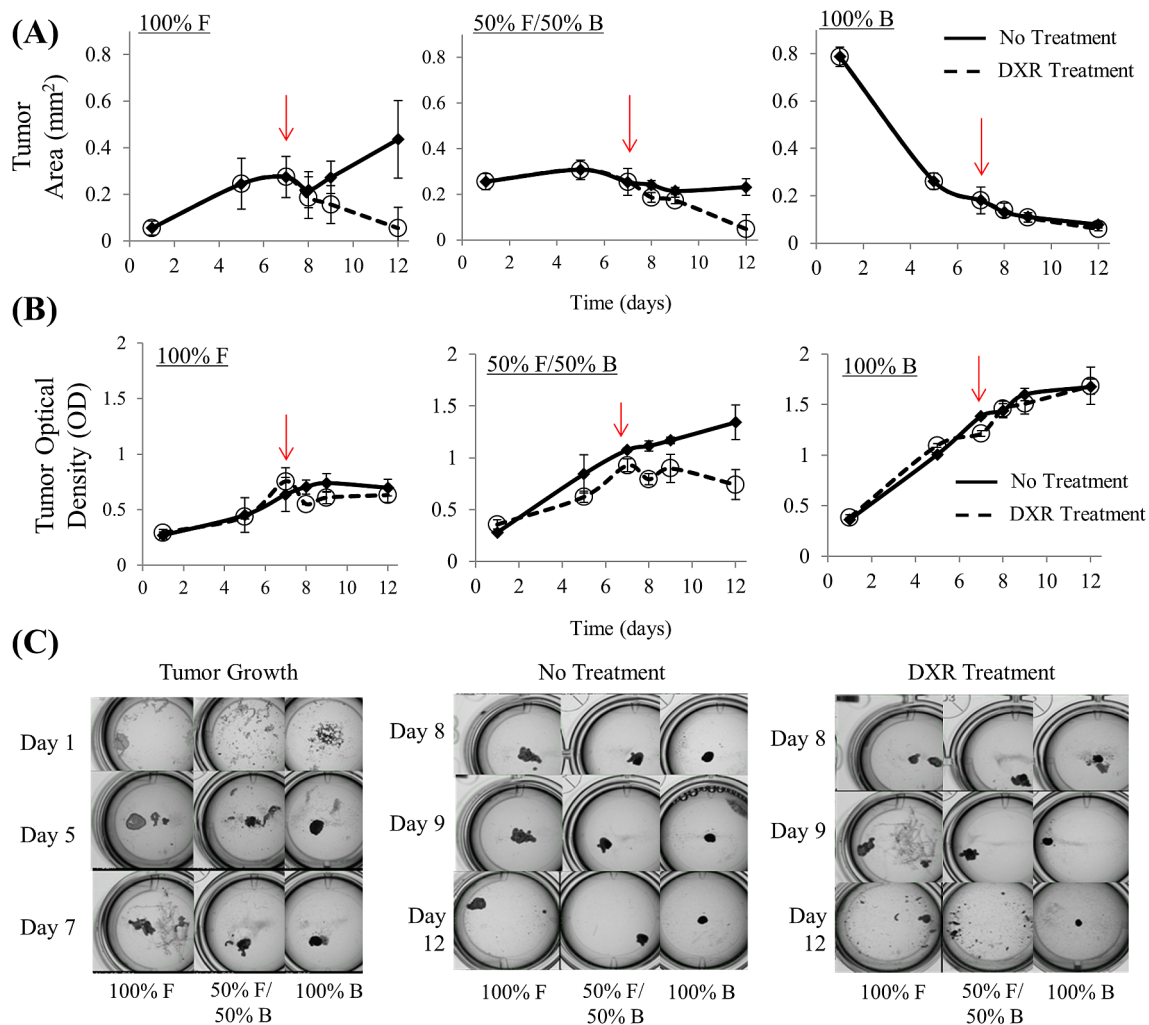


Figure 7 | Effect of doxorubicin treatment on 3D *in vitro* tumors: (A) Tumor area measurements and (B) Optical density measurements for 3D *in vitro* tumor composed of mono- and co-cultures of breast cancer and fibroblast cells. Arrows designate the start of doxorubicin (100 nM) treatment to 3D *in vitro* tumors. F = fibroblast and B = breast cancer cells.

obtain the comparable volume of the tumor spheres, the cells embedded in Matrigel™ had to be in culture for 7 days. Student T-test was performed on triplicates with 95% confidence at $p < 0.05$.

Monitoring of 3D *in vitro* tumor model. The 3D *in vitro* tumors were imaged using the GelCount™ instrument and tumor parameters such as diameter, optical density, and cross-sectional area were measured. The growth of the tumors was monitored by changes in area and optical density for 7 days. Then, the *in vitro* tumors were treated with doxorubicin (100 nM) the changes in area and optical density were compared to non-treated 3D *in vitro* tumors. The Gelcount™ instrument uses visible (i.e full spectrum) light to generate images and form the optical density values. ImageJ Analysis was used to quantify GelCount™ images.

1. Talukdar, S. *et al.* Engineered silk fibroin protein 3D matrices for in vitro tumor model. *Biomaterials* **32**, 2149–2159 (2011).
2. Yamada, K. M. & Cukierman, E. Modeling Tissue Morphogenesis and Cancer in 3D. *Cell* **130**, 601–610 (2007).
3. Leonard, F., Collnot, E. M. & Lehr, C. M. A three-dimensional coculture of enterocytes, monocytes and dendritic cells to model inflamed intestinal mucosa in vitro. *Mol. Pharm.* **7**, 2103–2119 (2010).
4. Zietarska, M. *et al.* Molecular description of a 3D in vitro model for the study of epithelial ovarian cancer (EOC). *Mol. Carcinog.* **46**, 872–885 (2007).
5. Cunha, C., Panseri, S., Villa, O., Silva, D. & Gelain, F. 3D culture of adult mouse neural stem cells within functionalized self-assembling peptide scaffolds. *Int. J. Nanomed.* **6**, 943–955 (2011).
6. Souza, G. R. *et al.* Three-dimensional tissue culture based on magnetic cell levitation. *Nat. Nanotechnol.* **5**, 291–296 (2010).
7. Vinci, M. *et al.* Advances in establishment and analysis of three-dimensional tumor spheroid-based functional assays for target validation and drug evaluation. *BMC Biol.* **10**, 29 (2012).

8. De Kruijff, E. M. *et al.* Tumor-stroma ratio in the primary tumor is a prognostic factor in early breast cancer patients, especially in triple-negative carcinoma patients. *Breast Cancer Res. Treat.* **125**, 687–696 (2011).
9. Downey, C. L. *et al.* The prognostic significance of tumour-stroma ratio in oestrogen receptor-positive breast cancer. *Br. J. Cancer* **110**, 1744–1747 (2014).
10. Shaw, K. M., Wrobel, C. & Brugge, J. Use of Three-Dimensional Basement Membrane Cultures to Model Oncogene-Induced Changes in Mammary Epithelial Morphogenesis. *J. Mammary Gland Biol.* **9**, 297–310 (2004).
11. Trédan, O., Galmarini, C. M., Patel, K. & Tannock, I. F. Drug Resistance and the Solid Tumor Microenvironment. *J. Natl. Cancer Inst.* **99**, 1441–1454 (2007).
12. Daquinag, A. C., Souza, G. R. & Kolonin, M. G. Adipose tissue engineering in three-dimensional levitation tissue culture system based on magnetic nanoparticles. *Tissue Eng. Part C Methods* **19**, 336–344 (2013).
13. Lee, J. S., Morrisett, J. D. & Tung, C. H. Detection of hydroxyapatite in calcified cardiovascular tissues. *Atherosclerosis* **224**, 340–347 (2012).
14. Dave, B. *et al.* Targeting RPL39 and MLF2 reduces tumor initiation and metastasis in breast cancer by inhibiting nitric oxide synthase signaling. *Proc. Natl. Acad. Sci. U. S. A.* **111**, 8838–8843 (2014).
15. Grantab, R. & Tannock, I. Penetration of anticancer drugs through tumour tissue as a function of cellular packing density and interstitial fluid pressure and its modification by bortezomib. *BMC Cancer* **12**, 214 (2012).
16. Vargo-Gogola, T. & Rosen, J. M. Modelling breast cancer: one size does not fit all. *Nat. Rev. Cancer* **7**, 659–672 (2007).
17. Kim, J. B., Stein, R. & O'Hare, M. J. Three-dimensional in vitro tissue culture models of breast cancer-- a review. *Breast Cancer Res. Treat.* **85**, 281–291 (2004).
18. de Kruijff, E. M. *et al.* Tumor-stroma ratio in the primary tumor is a prognostic factor in early breast cancer patients, especially in triple-negative carcinoma patients. *Breast Cancer Res. Treat.* **125**, 687–696 (2011).



19. Wang, K. *et al.* Tumor-stroma ratio is an independent predictor for survival in esophageal squamous cell carcinoma. *J. Thorac. Oncol.* **7**, 1457–1461 (2012).
20. Dekker, T. J. A. *et al.* Prognostic significance of the tumor-stroma ratio: validation study in node-negative premenopausal breast cancer patients from the EORTC perioperative chemotherapy (POP) trial (10854). *Breast Cancer Res. Treat.* **139**, 371–379 (2013).
21. Tlsty, T. D. & Hein, P. W. Know thy neighbor: stromal cells can contribute oncogenic signals. *Curr. Opin. Genet. Dev.* **11**, 54–59 (2001).
22. Krause, S., Maffini, M. V., Soto, A. M. & Sonnenschein, C. A novel 3D in vitro culture model to study stromal-epithelial interactions in the mammary gland. *Tissue Eng. Part C Methods* **14**, 261–271 (2008).
23. Morales, J. & Alpaugh, M. Gain in cellular organization of inflammatory breast cancer: A 3D in vitro model that mimics the in vivo metastasis. *BMC Cancer* **9**, 462 (2009).
24. Montanez-Sauri, S. I., Sung, K. E., Berthier, E. & Beebe, D. J. Enabling screening in 3D microenvironments: probing matrix and stromal effects on the morphology and proliferation of T47D breast carcinoma cells. *Integr. Biol. (Camb)* **5**, 631–640 (2013).
25. Bauer, J. A. *et al.* RNA interference (RNAi) screening approach identifies agents that enhance paclitaxel activity in breast cancer cells. *Breast Cancer Res.* **12**, R41 (2010).
26. Szot, C. S., Buchanan, C. F., Freeman, J. W. & Rylander, M. N. 3D in vitro bioengineered tumors based on collagen I hydrogels. *Biomaterials* **32**, 7905–7912 (2011).
27. Stevenson, C. S., Marshall, L. A. & Morgan, D. W. *In Vivo Models of Inflammation: Volume 1*. (Springer London, Limited, 2006).
28. Seo, B. R., DelNero, P. & Fischbach, C. In vitro models of tumor vessels and matrix: Engineering approaches to investigate transport limitations and drug delivery in cancer. *Adv. Drug Del. Rev.*
29. Netti, P. A., Berk, D. A., Swartz, M. A., Grodzinsky, A. J. & Jain, R. K. Role of Extracellular Matrix Assembly in Interstitial Transport in Solid Tumors. *Cancer Res.* **60**, 2497–2503 (2000).
30. Ong, S.-M. *et al.* Engineering a scaffold-free 3D tumor model for in vitro drug penetration studies. *Biomaterials* **31**, 1180–1190 (2010).
31. Timm, D. M. *et al.* A high-throughput three-dimensional cell migration assay for toxicity screening with mobile device-based macroscopic image analysis. *Sci. Rep.* **3** (2013).
32. Haisler, W. L. *et al.* Three-dimensional cell culturing by magnetic levitation. *Nat. Protoc.* **8**, 1940–1949 (2013).
33. Lee, G. Y., Kenny, P. A., Lee, E. H. & Bissell, M. J. Three-dimensional culture models of normal and malignant breast epithelial cells. *Nat. Methods* **4**, 359–365 (2007).

Acknowledgments

HJ, BD and BG acknowledge the financial support from Susan G. Komen PDF12229449 Award and BG, FL and SS thank NIH U54CA143837 and NIH 1U54CA151668-01.

Author contributions

B.G., G.S. and B.D. are responsible for conceptual idea. H.J., J.G. and F.L. collected the data. B.G., H.J. and F.L. wrote the main manuscript text and H.J., F.L., B.G. and S.S. prepared figures. All authors reviewed the manuscript.

Additional information

Competing financial interests: The authors declare no competing financial interests.

How to cite this article: Jaganathan, H. *et al.* Three-Dimensional *In Vitro* Co-Culture Model of Breast Tumor using Magnetic Levitation. *Sci. Rep.* **4**, 6468; DOI:10.1038/srep06468 (2014).



This work is licensed under a Creative Commons Attribution-NonCommercial-NoDerivs 4.0 International License. The images or other third party material in this article are included in the article's Creative Commons license, unless indicated otherwise in the credit line; if the material is not included under the Creative Commons license, users will need to obtain permission from the license holder in order to reproduce the material. To view a copy of this license, visit <http://creativecommons.org/licenses/by-nc-nd/4.0/>